

UC San Diego

UC San Diego Previously Published Works

Title

Low-cost mobile air pollution monitoring in urban environments: a pilot study in Lubbock, Texas

Permalink

<https://escholarship.org/uc/item/1m11q245>

Journal

Environmental Technology, 39(12)

ISSN

0959-3330

Authors

McKercher, Grant R
Vanos, Jennifer K

Publication Date

2018-06-18

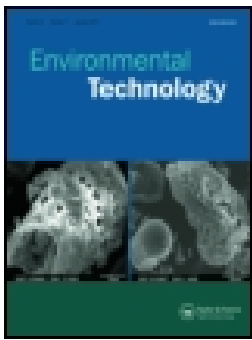
DOI

10.1080/09593330.2017.1332106

Copyright Information

This work is made available under the terms of a Creative Commons Attribution-NonCommercial-NoDerivatives License, available at <https://creativecommons.org/licenses/by-nc-nd/4.0/>

Peer reviewed



Low-cost mobile air pollution monitoring in urban environments: a pilot study in Lubbock, Texas

Grant R. McKercher & Jennifer K. Vanos

To cite this article: Grant R. McKercher & Jennifer K. Vanos (2017): Low-cost mobile air pollution monitoring in urban environments: a pilot study in Lubbock, Texas, Environmental Technology, DOI: [10.1080/09593330.2017.1332106](https://doi.org/10.1080/09593330.2017.1332106)

To link to this article: <http://dx.doi.org/10.1080/09593330.2017.1332106>

 View supplementary material 

 Accepted author version posted online: 17 May 2017.
Published online: 05 Jun 2017.

 Submit your article to this journal 

 Article views: 7

 View related articles 

 View Crossmark data 



Low-cost mobile air pollution monitoring in urban environments: a pilot study in Lubbock, Texas

Grant R. McKercher and Jennifer K. Vanos

Department of Geosciences, Texas Tech University, Lubbock TX, USA

ABSTRACT

The complex nature of air pollution in urban areas prevents traditional monitoring techniques from obtaining measurements representative of true human exposure. The current study assessed the capability of low-cost mobile monitors to acquire useful data in a city without a monitoring network in place (Lubbock, Texas) using a bicycle platform. The monitoring campaign resulted in 30 days of data along a 13.4 km fixed concentric route. Due to high sensitivities to airflow, the apparent wind velocity was accounted for throughout the route. The data were also normalized into percentiles in order to visualize spatial patterns.

The highest estimated pollution levels were located near frequently busy intersections and roads; however, sensor issues resulted in lower confidence. Additional research is needed concerning the appropriate use of low-cost metal oxide sensors for citizen science applications, as measurements can be misleading if the user is unaware of sensors specifications. The simultaneous use of several low-cost mobile platforms, rather than a single platform, as well as the use of high-end cases, are recommended to create a more robust spatial analysis. The issues addressed from this research are important to understand for accurate and beneficial application of low-cost gaseous monitors for citizen science.

ARTICLE HISTORY

Received 28 January 2017
Accepted 1 May 2017

KEYWORDS

Air pollution; monitoring;
low-cost; sensors; traffic;
spatial analysis

1. Introduction

Near-roadway air pollution related to heavy volumes of traffic can be dynamically complex, varying greatly within 100 m of a particular roadway [1–3], while distances between monitors in established urban networks are generally 1–10 km. Consequently, the small spatial and temporal scales at which humans are exposed are inconsistent with measurements from current monitoring networks.

The more recent use of mobile air pollution monitors has often found large differences between personal measurements and ambient monitoring station observations. For example, measured personal exposure to nitrogen dioxide gas (NO₂) (a common indicator of roadway air pollution) is often significantly higher near heavy traffic than the nearby monitoring station [4]. This discrepancy occurs because ambient measurements are intended to be representative of a local geographical area; however, the typical locations of ambient air-quality monitors are not always in close proximity to major pollutant sources [5,6]. Therefore, ambient monitors cannot represent the smaller micro-scale changes in air pollution that exist throughout urban areas and true human exposures are unknown [7,8].

It has been shown that people who spend more time near large roadways experience negative health effects [9], and in 2007 it was found that in the U.S., this affected population totaled approximately 45-million people [10]. A later study published similar numbers, where approximately 16% of U.S. housing units were located within 300 ft of a major highway, railroad, or airport (approx. 48 million people) [11]. Specifically, UFP (ultra-fine particles with a diameter 0.1 μm or less), NO (nitric oxide), and CO (carbon monoxide) concentrations have been found an order of magnitude higher near freeways than on residential streets [12], thus people nearest roadways with greater traffic volume are likely at greater risk.

Small, low-cost air pollution monitors have the ability to improve or supplement the spatial and temporal resolution of current data and expand monitoring to locations where there are no air pollution observations [5,6,8]. Two methods for supplementary monitoring with low-cost monitors include the development of high-density sensor networks (e.g. Aairsensa [13]) and the development of commercially available mobile monitors that wirelessly transmit data for crowdsourcing (e.g. Smart Citizen [14]). Although there is a lack of concrete information on the effective use of such sensors by

CONTACT Jennifer K. Vanos  jkvanos@ucsd.edu

 Supplemental data for this article can be accessed at <https://doi.org/10.1080/09593330.2017.1332106>.

© 2017 Informa UK Limited, trading as Taylor & Francis Group

individuals and communities, specific vulnerable populations in urban areas can benefit from these sensor systems (e.g. child exposure [15,16], environmental justice [17]).

Further, efforts from citizen and joint academic-community science initiatives can help identify environmental health problems associated with air quality in urban areas. Yet, in order for small, low-cost monitoring data to influence real action, it must be accurate. Unfortunately, there remains a gap between technological development and successful use of newer technologies within communities of proactive decision-making [18]. With respect to air-quality sensors, McKercher [19] compared various available gaseous monitors, highlighting common issues in cost, precision, sensor sensitivities, and applicability for different purposes, including citizen science. The advent of cheap, accurate, commercially available air pollution monitors has immense potential, yet real-world application of such sensors by average citizens is relatively unstudied.

Therefore, the current research study employed low-cost mobile air pollution monitors on a bicycle platform with an objective to utilize the monitors in a manner similar to the average ‘citizen scientist’. The main goal of performing this study in Lubbock, Texas, was to assess the capabilities of low-cost mobile monitors to acquire useful, actionable data in a city without a monitoring network in place. Lubbock, TX (population estimated to exceed 300,000 [20]) is one of many small-to-medium sized cities lacking regulation-grade air pollution monitors. The nearest regulatory monitor to Lubbock is over 100 miles away, thus common ambient air pollution levels are unknown and challenging to estimate.

2. Experimental

2.1. Study design

A fixed-site station (FSS) was installed on an open, grass field west of Texas Tech University (33.578, -101.895), 30 m from the nearest roadway (19th Street), which commonly experiences medium to heavy traffic. This location was chosen because of proximity to two organizations (TTU campus and Covenant Hospital) with large, potentially vulnerable populations (i.e. students, elderly). The FSS included advanced meteorological instruments (Campbell Scientific, Inc) that measured temperature and relative humidity, solar radiation, wind speed, and wind direction enclosed within a small chain-link cage. For further information including a local scale overhead view of the study area and a labeled photo of the FSS, see Supporting Information (SI) pages S2–S4.

The Smart Citizen Kit (SCK) low-cost environmental monitor (designed for citizen science) measures CO/NO₂, temperature, humidity, light intensity, and sound levels. The SCK has a battery lifetime of four hours and may be programmed to sample at various rates (e.g. 25, 5, or 1 s). The CO/NO₂ sensor (MiCS-4514) is a metal oxide sensor (MOS) that outputs measurements of resistance ($K\Omega$) corresponding to real gas concentrations. Currently, no formal studies of SCK performance have been published in peer reviewed scientific literature, however, one evaluation comparing SCK CO/NO₂ responses to a reference monitor has been performed [21] – likely using a similar configuration, but without cases – where findings indicated CO data was reliable, while NO₂ was not. The MiCS-4514 contains two sensor chips with individual heaters and metal oxide layers responsive to either reducing (RED) or oxidizing (OX) gases [22]. The resistance of the RED sensor chip decreases in relation to CO gas, while the resistance of the OX sensor chip increases in relation to NO₂. Ideally, a decrease in CO resistance corresponds to an increase in true CO concentrations, while an increase in NO₂ resistance corresponds to an increase in true NO₂ concentrations. See SI page S6 for generalized graphs of these relationships. For specific information on SCK components, see SI page S5.

For mobile monitoring, an SCK was strapped to each of the researcher’s wrists (see Figure 1(A,B)) and a GPS was mounted onto the handlebars. Separately, a third SCK was mounted onto the FSS. The experiment was designed to control for confounding factors such as weather and traffic, while achieving a consistency repeatable on multiple days per week. For example, the mobile platform was deployed on weekdays (with the exception of two days) between 15:00 and 17:00 when air temperatures were above 70°F (21.1°C) and skies were mostly clear. In total, mobile data were collected on 30 days. For a complete list of the monitoring days, see SI page S7.

The experimental route was designed so that data may be collected at varying distances from the FSS. It consisted of a single fixed path made up of three complete loops: a small, medium, and large loop (see Figure 2). The route followed a concentric pattern through multiple micro-environments (e.g. suburban neighborhoods, business corridors, and bicycle paths) for approximately 8.3 miles (13.4 km) starting and finishing at the same position. Each ride lasted about 40 min including stops where appropriate (e.g. intersections).

Multiple configurations of each SCK (1, 2, and/or 3) were used throughout the mobile monitoring campaign, consisting of three periods: Period A, B, and C (see Table 1). For the majority of the study, SCK1 was enclosed within a plastic 3D-printed case with open air

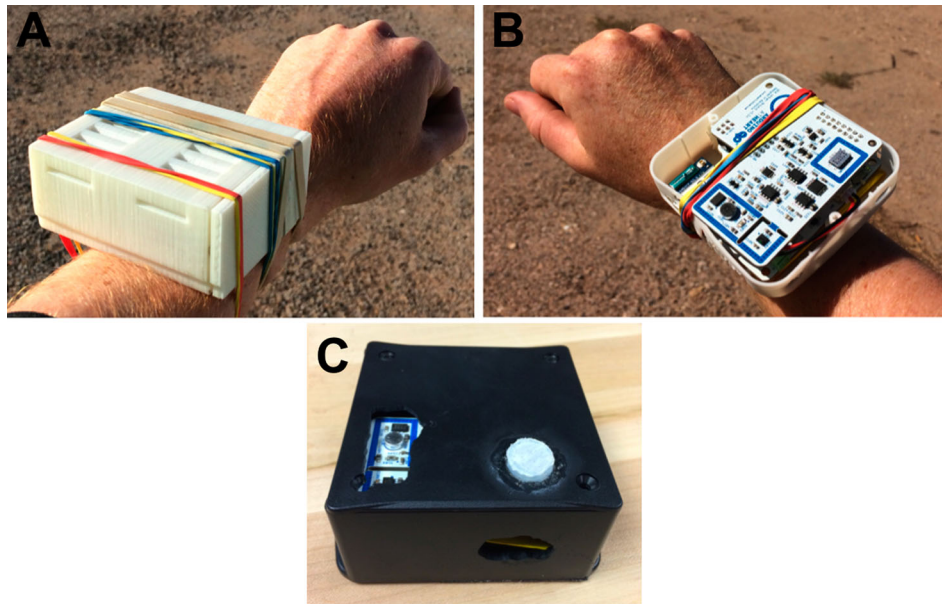


Figure 1. (A) SCK1 inside a 3D printed case on the researcher's left wrist. (B) SCK2 in an open battery holder on the researcher's right wrist. (C) SCK3 in one of the two cases purchased from Polycase outfitted with a PTFE membrane over the air pollution sensor.

ventilation (see Figure 1(A)). The initial reason for ventilation was to eliminate sampling issues related to lag, maximizing the amount of air passing over the sensor. The case also served to protect the monitor from external damage. However, for reasons discussed later, during the final five sampling days (27 April 2016–6 May 2016), SCK2

and SCK3 were housed and covered by plastic cases purchased online (Polycase). The cases were cut open over the air pollution sensor and a Teflon tube was inserted and glued into place with a 2 μm PTFE (Polytetrafluoroethylene) membrane filter covering the hole (see Figure 1(C)).

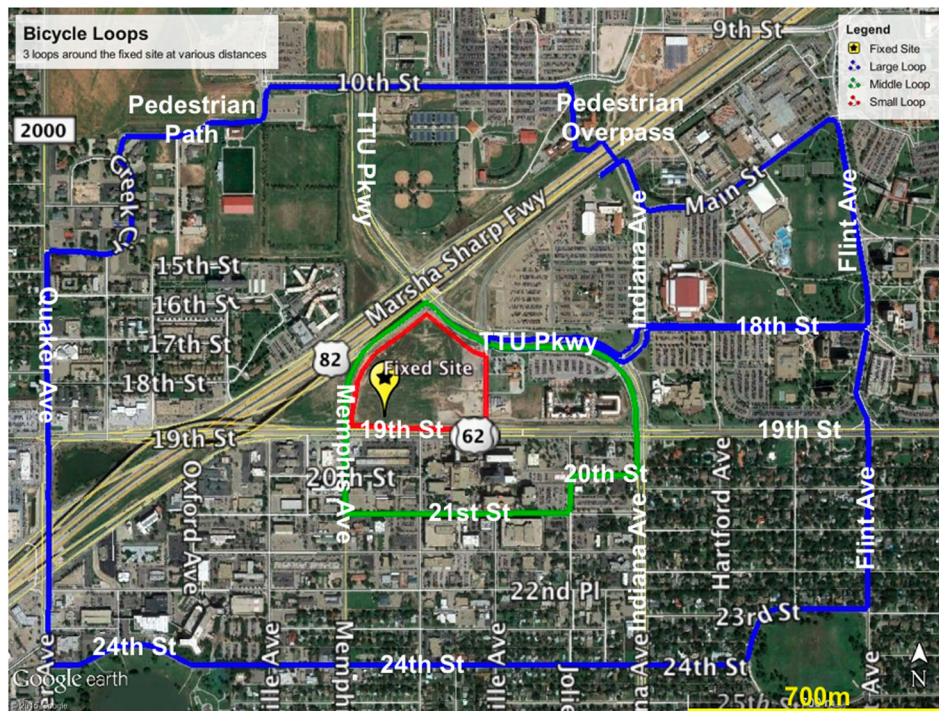


Figure 2. The bicycle route for the mobile deployment. All loops were a part of a single continuous ride. The pin is at the location of the FSS. Map from Google Earth [36].

Table 1. Comparison of the mobile data collection periods.

Period	First date	Last date	Number of sampling days	SCK(s)	Cases
A	2/10/15	20/2/16	8	SCK1 ^a	SCK1 only ^b
B	2/3/16	15/4/16	17	SCK1,2,3	SCK1 only ^b
C	27/4/16	6/5/16	5	SCK1,2,3	ALL ^c

Note: See SI page S7 for the expanded and more detailed version.

^aDue to funding constraints, only SCK1 was used.

^bSCK1 in 3D-printed case, SCK2,3 without cases.

^cSCK1 in 3D-printed case, SCK2,3 in plastic cases with PTFE membranes covering the MOS sensor.

2.2. Testing the SCKs

To quantify differences between the three SCK air pollution sensors, multiple indoor baseline tests were performed. The baseline tests involved extended periods (e.g. 60–120 min) of stationary indoor monitoring in a closed room.

Also, a series of bump tests were completed in order to test SCK responsiveness to CO and NO₂ gases, although we recognize that these tests would not be possible by average citizens. For the bump tests, a tabletop chamber was built from a 5.7 L clear plastic bin connected with tygon tubing to a gas cylinder regulator and a small cylinder of calibration gas. In total, three CO gas cylinders (2, 20, and 35 ppm) and one NO₂ gas cylinder (1 ppm) were used. Bump tests were performed with each CO and NO₂ gas indoors during multiple occasions throughout March, April, and May, 2016. Typically, all three SCKs were closed within the chamber and each gas cylinder was used at 0.5 LPM for 2–5 min. Gases were allowed to escape the chamber from a small hole on the opposite end. For detailed examples of the bump tests, see SI pages S9–S10.

To test the air pollution sensors' responses to airflow, a laboratory test was performed with a small indoor fan, directing air at two different speeds ('low' and 'high') towards the three SCK sensor boards. The average wind speeds from the two fan settings were estimated to be 1.5 and 3.5 ms⁻¹ respectively using a cup anemometer over a series of several minutes. Additionally, an outdoor test was performed, measuring the effect of activity speed on SCK air pollution measurements. A detailed description of the outdoor airflow test is included from SI page S12.

2.3. Methods for analysis

There were three main sources of data for the mobile experiment: (1) the SCKs, (2) the FSS, and (3) the GPS. First, all raw data were separately quality controlled and processed according to the source. Next, the SCK and FSS data were averaged, thus smoothing the data and

dampening noise effects. For example, 1 or 5 s SCK data were averaged to 25 s intervals and 5 s FSS data were averaged to 1 min intervals. The SCK and FSS timestamps nearest to each GPS time were then separated and matched. Within this process, a positive linear trend in the NO₂ data associated with the sensor warmup was removed with statistical detrending. See SI pages S14 and S15 for more detail regarding these processes.

The horizontal components of the wind velocity were used to calculate the wind vector (V_w) and the horizontal components of the activity motion were used to calculate the activity vector (V_a). The angle between the wind and activity vectors was calculated using Equation (1) and the apparent wind velocity experienced by a cyclist (V_r) was found using Equation (2), where V_w is wind speed, V_a is activity speed, and α is the angle between the wind direction and activity motion. Equation (1) is derived from the law of cosines where the angle is shifted by π (180°).

$$\alpha = \arccos\left(\frac{\vec{V}_a \cdot \vec{V}_w}{|\vec{V}_a| \cdot |\vec{V}_w|}\right), \quad (1)$$

$$V_r = \sqrt{(V_a^2 + V_w^2 - (2V_a V_w \cos(\pi - \alpha)))}. \quad (2)$$

2.4. Spatial and statistical analyses

Due to multiple issues with the SCKs monitors (which are discussed in detail in upcoming sections) the following spatial and statistical methods were called upon in order to appropriately analyze the mobile data in this study. To view changes in air pollution data spatially, matched GPS and SCK data were plotted on a local tangent plane. Using point locations, maps were created showing locations of higher and lower estimated air pollution levels based upon the SCK resistance data. In the context of this paper, the highest 10th percentile refers to the highest 10% of *evenly* distributed data. To normalize the data so that true spatial patterns would be revealed, the highest 10th percentile (corresponding to higher air pollution concentrations) were separated from each day and plotted all together as points. These plots displayed the locations of the lowest 10% of the CO resistances and highest 10% of the NO₂ resistances for each day, overlaid for all days in which SCK1 ($n = 26$) and SCK2 ($n = 22$) were used; therefore, the locations with the greatest number of points corresponded to a greater frequency of that location having higher air pollution than other locations.

Further spatial analysis was performed on the clustering of the points from the CO and NO₂ highest 10th

percentiles. Using ArcGIS 10.1, point density layers were calculated as heatmaps, visualizing the areas in which high air pollution values were most frequently and densely located. This was performed for both mobile monitors: SCK1 and SCK2. Following the creation of the heatmaps, data points within the greatest densities were selected, separated into new files, and statistically compared against the entire 10th percentile dataset ($p < .05$).

Pearson correlations were calculated and significance testing performed between various measured quantities. For the significance tests, data from each SCK were normalized from 0 to 1 to remove inter-SCK biases and separate ‘post-hoc’ t -tests were performed between all variables. By applying a null hypothesis that each pair of variables had equal means, significance testing was also performed between sampling days in which SCK2 and SCK3 were open (Periods A and B) and covered with plastic cases (Period C) ($p < .05$).

3. Results and discussion

3.1. SCK tests

Results from the indoor baseline tests were noticeably different between the three SCKs. For example, SCK1 generally reported much higher CO /NO₂ resistance values than both SCK2 and SCK3 (positive bias). Also, there were small differences between SCK2 and SCK3, indicating out-of-the-box variability. Furthermore, results showed differences between the days in which similar baseline tests were performed, which may be related to individual characteristics and errors of each sensor. See SI pages S8–S9 for more description and tables of these results. Together, these issues made it challenging to trust data from individual SCKs; however, by normalizing the data, results from the monitoring campaign could be compared between SCKs.

The bump tests showed that increasing concentrations of CO gas had only a minor effect on CO resistance output for all three SCKs. However, sealing the top of the chamber caused an immediate decrease in resistance and when the top of the chamber was opened, the resistance measurements returned to baseline values. It seems that the sensor resistances were more heavily impacted by the opening and closing of the chamber. This may highlight an issue with the MiCS sensors themselves (i.e. cross-sensitivities or airflow dependencies [23]). The NO₂ bump test showed a positive resistance response to NO₂ gas, which was increasing in time. It is unknown if the increasing NO₂ response was due to the fact that gas was allowed to escape or if it was a characteristic of the sensor (i.e.

sensor warmup). See SI pages S9–S10 for data and more information on the bump tests.

In general, the SCKs responded to gases in the expected direction (decreasing resistance was associated with increasing CO and increasing resistance when exposed to NO₂), however, given the variabilities found from the baseline tests and challenges of interpreting bump test results, calibration curves could not be developed for the CO /NO₂ sensors. The SCK tests resulted in a general lack of response to known concentrations of CO and a more noticeable, increasing response to NO₂ gas (see figures on SI pages S9–S10). These results were not useful to relate the raw resistance data to the true calibration gas concentrations, unlike the results of the outdoor evaluations reported by the South Coast Air Quality Management District’s Air Quality Sensor Performance Evaluation Center (AQ-SPEC) [21], which provided helpful information about the reliability of the SCK.

Controlled airflow from the fan resulted in an immediate positive response for both CO and NO₂ resistances, however, there was not a significant change when the speed was switched from ‘low’ (1–1.5 ms⁻¹) to ‘high’ (2.5–4.5 ms⁻¹). The fan caused SCK temperatures to decrease about 4°C, which agrees with a previous study that reported a maximum temperature drop of 8°C due to airflow generated from a fan at speeds near 6.6 ms⁻¹ [24]. The data from this test are shown on SI page S11.

The amount of wind passing over each sensor board is an important factor when using MOS air pollution sensors. The use of MOS sensors on a bicycle platform likely results in significant inflation of the resistance measurements, especially when the activity velocity is high (see outdoor activity test results on SI page S12). Increased airflow across the MiCS-4514 alters the heated layer temperature [23] and because MOS sensors rely on metal oxide conductivity to make measurements, a change in temperature causes a corresponding change in output resistance. Henceforth, it is crucial for MOS air pollution sensors to have well-designed protection (i.e. case and Teflon membrane) to shield components from airflow, especially when used on a bicycle platform [23] or in windy environments.

The lack of attention that the airflow issue has received in scientific literature and sensor documentation has made measurements from devices such as the SCK somewhat misleading. Given the applications of the SCK (citizen science and crowdsourcing) and the challenges experienced in this study, the SCK is not recommended for air pollution monitoring in a city without a reference monitoring network, especially in high winds. It is possible that similar sensors have been able to report accurate air pollution measurements in laboratory sensor evaluations with low airflow (e.g. EPA Sensor Evaluation

Report [25]), yet tests of these sensors in outdoor environments are needed to truly assess their ability to observe ambient air pollution. Ideally, in order to evaluate the performance of the SCKs, a comparison with an outdoor ambient monitor should have been completed, such as AQ-SPEC [21]. There were potential flaws with the indoor bump tests with calibration gases, but because CO data have been proven fairly accurate to ambient outdoor concentrations [21], the field results from this study have some validity.

If the SCK or similar monitors are frequently calibrated with an outdoor reference monitor and properly protected from the airflow, it is possible that they may convey more impactful findings. A categorical system is necessary to separate instruments that are sufficient for accurate measurements on their own and monitors that require frequent calibrations or collocation with reference analyzers [19].

3.2. Mobile monitoring campaign

GPS points were plotted at the locations of daily lowest 10% CO resistances (highest estimated true CO levels) and daily highest 10% NO₂ resistances (highest estimated true NO₂ levels). By separating the data into percentiles, daily variations (as found in the baseline tests) were removed and by normalizing the individual SCK data, out-of-the-box differences were accounted for.

Further influences from airflow were minimized due to the large number of samples and quantified using statistical comparisons to measured wind velocity at the FSS (SCK3) and apparent wind velocity along the monitoring route (SCK1,2). SI pages S15–S16 show an example of one day of data.

The left maps on Figure 3 are point density heatmaps of the daily lowest 10% of CO resistances, which cluster to several specific regions. These regions were similar between SCK1 and SCK2, however, the SCK2 point densities were generally lower in magnitude because SCK2 was used on fewer days. Most importantly, the regions of interest for both mobile SCKs have been identified near or along intersections of roads that commonly experience moderate to heavy traffic. Table 2 lists statistics from each intersection subset compared to the 10th percentile as a whole. The mean CO resistances at two specific intersections, 19th St. & Knoxville Ave. and TTU Pkwy. & Knoxville Ave. were significantly lower than the 10th percentile mean for both SCK1 and SCK2 (see Table 2). These locations were most frequently associated with significantly low CO resistances, which may have been due to significantly higher true air pollution levels.

The maps on the right in Figure 3 show point density heatmaps of the daily highest 10% of NO₂ resistances. High NO₂ levels were most frequently recorded near one intersection in common with the previous CO analysis (TTU Pkwy. & Indiana), however, the other locations of

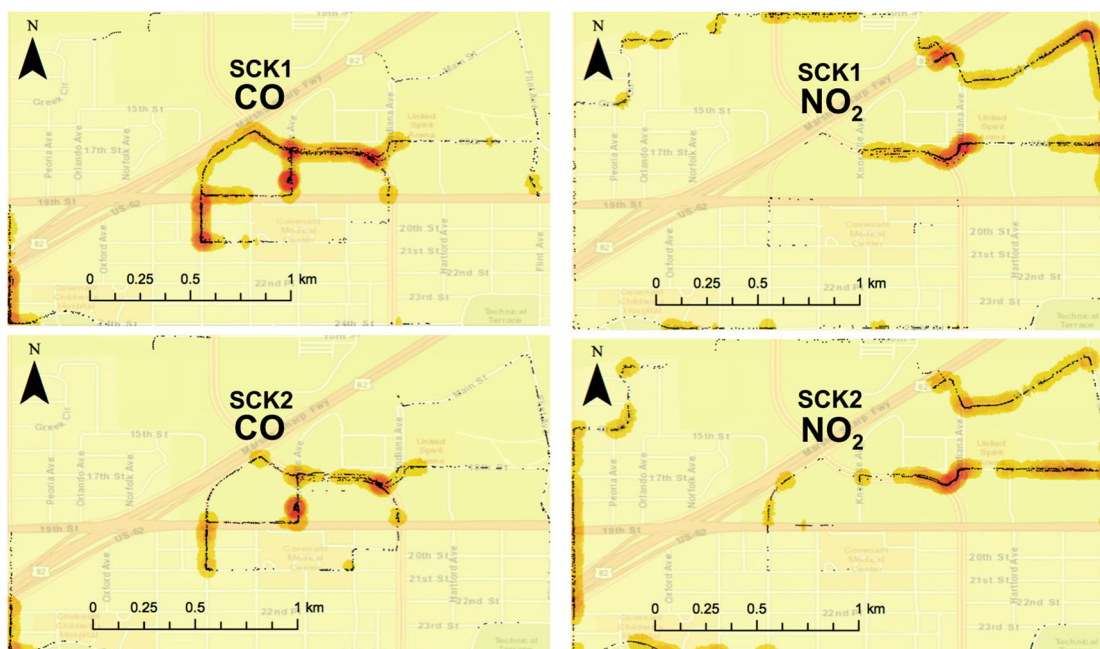


Figure 3. Point density heatmaps showing areas of highest estimated CO and NO₂ measured by SCK1 (top) and SCK2 (bottom). Points on left plots show GPS locations of the lowest 10% CO resistances, overlaid for all days for SCK1 ($n = 26$) and SCK2 ($n = 22$) and points on right plots show GPS locations of the highest 10% NO₂ resistances, overlaid for all days for SCK1 ($n = 26$) and SCK2 ($n = 22$). Map underlay from Google Earth [36].

Table 2. Descriptive statistics of CO compared between the lowest 10th percentile and selections of subsets at specific intersections where point densities were highest.

Dataset	SCK1 CO(KΩ) Mean±SD	SCK2 CO(KΩ) Mean±SD
10th percentile	589±117	373±77
19th St. and Knoxville Ave.	545±105*	351±89*
19th St. and Memphis Ave.	594±104	364±80
21st St. and Memphis Ave.	609±77	NA
24th St. and Quaker Ave.	653±89*	384±71
TTU Pkwy. and Indiana Ave.	541±118*	371±66
TTU Pkwy. and Knoxville Ave.	556±122*	353±89*

*Significant difference from the 10th percentile ($p < .05$).

NA – data subset not created for comparison.

interest did not match between the two pollutants. Also, the NO₂ data indicated slight differences between SCK1 and SCK2. Clusters of SCK1 points were found in three regions in the northeastern corner of the large loop, while much of the SCK2 clustering was located along the western edge of the large loop (Quaker Ave.). Table 3 includes statistical descriptions of the NO₂ resistances from the subsets at each of the locations with the highest point density. It was found that within the 10th percentile dataset of SCK1 resistances, levels were significantly higher in the cluster of measurements taken on the southern side of a pedestrian overpass across Highway 82. For SCK2, levels were significantly higher for subsets at two intersections, TTU pkwy. & Indiana Ave. and Main St. & Indiana Ave. (see Table 3), which commonly have moderate to high traffic volumes. Both of these intersection locations indicate that high traffic may have been a main factor in NO₂ measurements.

Considering the airflow test results, there were two important reasons why these spatial results may be justified. First, many dense regions of high concentrations (or apparent enhanced concentrations) were shared between both CO and NO₂ analyses, which demonstrated a mismatch between the expected response to airflow and sensor characteristics. Second, the regions with consistently higher apparent wind velocity did not correspond with the regions of the highest NO₂.

Table 3. Descriptive statistics of NO₂ compared between the highest 10th percentile and selections of subsets at specific intersections where point densities were highest.

Dataset	SCK1 NO ₂ (KΩ) Mean±SD	SCK2 NO ₂ (KΩ) Mean±SD
10th percentile	98±124	47±16
Flint Ave. and 18th St.	69±34	45±18
Main St. and Flint Ave.	114±149	NA
Overpass	195±197*	NA
TTU Pkwy. and Indiana Ave.	87±60	59±18*
Main St. and Indiana Ave.	NA	56±14*
Quaker Ave. and Highway 82	NA	45±13
Quaker Ave. and 19th St.	NA	42±13

*Significant difference from the 10th percentile ($p < 0.05$)

Note: NA – data subset not created for comparison.

These spatial results cannot confirm that the presence of idling vehicles at intersections or high traffic volumes were the cause of such spatial patterns, however, the results somewhat agree with the inclination. Spatial results were only achievable in this study because of the high number of samples over a single, specified route, which was inspired by previous studies using bicycle platforms (e.g. [26–28]) because it guaranteed sufficient spatial and temporal coverage and allowed for a general analysis of local peak concentrations over a specified area. Also, given that airflow was, on many occasions, high in velocity near dense CO regions and low in velocity near dense NO₂ regions, results in this section are likely a result of true air pollution exposure.

3.3. Meteorological relationships

Pearson correlation coefficient values (r) were calculated for the entire mobile monitoring campaign (see SI page S13). Such data can indicate cross-sensitivities with environmental attributes, including weather and air pollution levels. This study found that both SCK temperature and FSS temperature were weak-to-moderately negatively correlated with CO and NO₂ resistances for all three SCKs. This result demonstrates the sensitivity of temperature on the conductive measurement technique of the MiCS air pollution sensor in which lower temperatures are related to increased sensor resistance similar to the relationship reported by SGX Sensortech [23]. Therefore, variations in daily air temperature between each monitoring day likely had an effect on air pollution measurements.

SCK3, which was mounted onto the FSS, reported CO /NO₂ resistances that were positively correlated with wind speed. Correlations between the mobile monitors (SCK1/SCK2) and V_r were also positive, yet less significant. These results align with the results from the airflow tests, which reported increased sensor resistances with wind speed. Additionally, a positive relationship was found between SCK3 CO and SCK3 NO₂ resistances, which may be caused by sensor cross-sensitivities to interfering gases. There was not a strong relationship between CO /NO₂ resistance and relative humidity, although humidity can alter the sensitivity and reactivity MOS sensors [23].

The statistical significance analyses between the three monitors demonstrated that means for most variables (including the normalized air pollution values) were significantly different between each individual SCK ($p < .05$). For example, normalized temperature measurements were significantly different between SCK1 and SCK2. However, it was found that normalized SCK1 temperature readings were significantly similar to the FSS wind speed measurements, which demonstrated

a relationship between daily wind speed and temperature of the mobile platform. Additionally, the significance tests found that normalized SCK3 temperature and normalized SCK3 NO₂ resistance were significantly similar. This result confirmed that the temperature of the device was significantly related to the MOS sensor characteristics.

Correlations between air pollution and local meteorology have been useful for previous researchers to identify trends. For example, it has been shown that temperature and wind speed were negatively correlated with near-road concentrations of UFP [29]. The current study reported a similar result, that CO /NO₂ resistances were negatively correlated with temperature. This relationship was much stronger for CO than NO₂. Although these correlations may be an artifact of the sensor technology, as indicated by the tests, the result fits well with the common notion that air pollution concentrations can be higher on warmer days (i.e. ozone [30]).

3.4. The impact of Teflon covers

The plastic cases with Teflon covers that were deployed on SCK2 and SCK3 during Period C successfully dampened the effect of airflow over the MOS sensors, resulting in lower mean resistances compared to Periods A and B when no cases and Teflon covers were used (see Table 4). Standard deviations were lower during Period C, indicating that the use of cases also decreased the variance of resistance values. Significance testing between the days with and without cases demonstrated that the normalized resistance values were significantly different ($p < .05$) depending on whether or not the cases were used (between Periods A/B and Period C). Also, normalized mean SCK temperatures were higher during Period C due to the shielding of airflow from the presence of the plastic case. It can be concluded that the cases were effective at decreasing the impact of airflow on SCK output.

3.5. Validity and limitations

This pilot study in Lubbock, Texas, provides a framework for future studies using mobile air pollution sensors in underserved cities (i.e. those without continuous air quality measurements) on a low budget. Due to the

lack of regulatory monitoring in Lubbock, Texas, the potential impact of roadway air pollution on human health is unknown. Although low-cost air pollution monitors have been useful for previous research in Lubbock [31], this study has determined that a single low-cost, mobile monitoring platform is not ideal for a study of the spatiotemporal behavior of near-roadway air pollutants in a city. Whether small, low-cost (and inherently less-accurate) air pollution monitors may still have value for research purposes is still a developing topic of interest [6]. A greater number of monitors or platforms working continuously and simultaneously over a larger area would more accurately assess an urban area's near-roadway air pollution. Because many repeated samples were recorded along the same route in this study, normalized spatial data were able to identify air pollution patterns; however, the authors acknowledge that using a slightly higher cost system (e.g. The Village Green Project [32]) in fewer locations would be a possible alternative. Such a method may employ a network of stationary monitors that are capable of obtaining longer periods of data, but they may be less informative of the local spatial tendencies of air pollution.

Budget, personnel, and equipment constraints limited what was able to be accomplished in the time period, yet the goal to assess the feasibility of low-cost, mobile monitoring by average citizens in real-world conditions was met. There are few available devices for low-cost monitoring [19], and the chosen monitor was not the most optimal device for mobile monitoring. A reliable monitoring platform with well-tested calibration procedures would have been ideal. Also, since only a single meteorological station was used, an assumption was made that weather conditions were constant throughout the study area. Further, lack of traffic volume data in Lubbock prevented true relationships between roadways and air pollution from being quantified. The greatest limitation was the lack of high-end laboratory calibration equipment, thus CO /NO₂ data were unable to be directly related to human health.

3.6. Future directions

The use and improvement of complete sensor systems and similar MOSs in carefully designed research is encouraged, but challenges faced during this study

Table 4. Comparison between mobile SCK data recorded with no cases (Periods A,B) and cases with Teflon covers (Period C).

	SCK2 CO(KΩ)	SCK3 CO(KΩ)	SCK2 NO ₂ (KΩ)	SCK3 NO ₂ (KΩ)	SCK2 (T°C)	SCK3 (T°C)
Periods A,B	564±105	423±82	36±10	45±20	23.0±2.5	24.5±2.5
Period C	376±43	255±76	32±12	25 ±12	25.8±1.9	30.8±3.5

indicate that average citizens – an intended audience of low-cost monitors – will not have the resources to correct or obtain useful results from misleading measurements. Low-cost devices similar to the SCK can have great value if proper precautions are taken (e.g. frequent calibration [5], firmware and/or physical components used to avoid meteorological influences [31], data processing quality control [32]). The issues identified in this study demonstrate where basic improvements can be made in the full-engineered sensor system (e.g. case, membrane filter, signal processing) that will advance the use of gaseous air quality monitors so that trusted outdoor data can be obtained by the average person in the future. In addition, this study's unique application of spatial analysis software is likely beyond the scope of most citizen scientists; however, if similar statistical techniques can be developed into a monitor's firmware, or if software can be provided by the manufacturer for post-processing to provide data visualization, then the intended purpose of these systems for citizen science may be achieved.

The proliferation of small, low-cost sensing technologies will continue due to the high number of applications, however, the current work highlights that low-cost air pollution sensing has various challenges to overcome before it becomes effective in solo research studies. Potential improvements that would combat such challenges may involve the standardization of calibration procedures and testing with integrated values specific for each monitor, as well as careful design of appropriate cases allowing pollutant penetration, but blocking wind. Techniques similar to those administered in this study are at the forefront of understanding personal exposure to air pollution in urban areas. For example, low-cost mobile monitors may become further enhanced to have uses for a wide range of pollutants at high density, providing data that helps refine existing air pollution models and the development of newer models [4]. Also, similar research may be used to influence citizens to change their behavior and follow cleaner routes [33,34]. For individuals with health ailments, experience with air pollution monitors may become essential to enhance their awareness and thus allow them to consciously avoid harmful exposure. Future results may be valuable resources for local city planners, health agencies, and other public decision makers [35], providing guidance for smarter urban growth and further independence from federal and state resources.

3.7. Supporting information

Supporting Information Available: Further information on the specifics in experimental design and materials

used are discussed in greater detail. Additionally, data from tests including the baseline tests, bump tests, and airflow tests are included with descriptions and figures. The SI also includes tables with data that correspond with the results section of this article. This material is available free of charge online via Figshare.

Acknowledgments

This work could not have been completed without multiple individuals who have contributed time and/or materials, including Wes Burgett (TTU National Wind Institute), Tingting Cao and Dr Jonathan Thompson (TTU Chemistry), and Dr Jennifer Salmond (University of Auckland, School of Environment). Also, large thanks goes to Dr Eric Bruning (TTU Atmospheric Science) for influencing code for the analyses.

Disclosure statement

No potential conflict of interest was reported by the authors.

Funding

A special thanks goes to Oakridge National Laboratories for providing the initial funding to make this project possible.

References

- [1] Karner AA, Eisinger DS, Niemeier DA. Near-roadway air quality: synthesizing the findings from real-world data. *Environ Sci Technol.* 2010;44:5334–5344.
- [2] Snyder EG, Watkins TH, Solomon PA, et al. The changing paradigm of air pollution monitoring. *Environ Sci Technol.* 2013;47:11369–11377.
- [3] Zhou Y, Levy JI. Factors influencing the spatial extent of mobile source air pollution impacts: a meta-analysis. *BMC Publ Health.* 2007;7:89.
- [4] Delgado-Saborit JM. Use of real-time sensors to characterise human exposures to combustion related pollutants. *J Environ Monit.* 2012;14:1824–1837.
- [5] Williams R, Kilaru V, Snyder E, et al. Air sensor guidebook, 2014. Available from: <https://nepis.epa.gov/Exe/ZyNET.exe/P100JDZI.TXT?ZyActionD=ZyDocument&Client=EPA&Index=2011+Thru+2015&Docs=&Query=&Time=&EndTime=&SearchMethod=1&TocRestrict=n&Toc=&TocEntry=&QField=&QFieldYear=&QFieldMonth=&QFieldDay=&IntQFieldOp=0&ExtQFieldOp=0&XmlQuery=&File=D%3A%5Czyfiles%5CIndex%20Data%5C11thru15%5CTxt%5C00000010%5CP100JDZI.txt&User=ANONYMOUS&Password=anonymous&SortMethod=h%7C-&MaximumDocuments=1&FuzzyDegree=0&ImageQuality=r75g8/r75g8/x150y150g16/i425&Display=hpfr&DefSeekPage=x&SearchBack=ZyActionL&Back=ZyActionS&BackDesc=Results%20page&MaximumPages=1&ZyEntry=1&SeekPage=x&ZyPURL>
- [6] Kumar P, Morawska L, Martani C, et al. The rise of low-cost sensing for managing air pollution in cities. *Environ Int.* 2015;75:199–205.
- [7] Baxter LK, Dionisio KL, Burke J, et al. Exposure prediction approaches used in air pollution epidemiology studies:

- key findings and future recommendations. *J Exp Sci Environ Epidemiol.* 2013;23:654–659.
- [8] Steinle S, Reis S, Sabel CE. Quantifying human exposure to air pollution—moving from static monitoring to spatio-temporally resolved personal exposure assessment. *Sci Total Environ.* 2013;443:184–193.
- [9] HEI, traffic-related air pollution: a critical review of the literature on emissions, exposure, and health effects; 2010. (Health Effects Institute Special Report 17).
- [10] Kimbrough S, Baldauf RW, Hagler GS, et al. Long-term continuous measurement of near-road air pollution in Las Vegas: seasonal variability in traffic emissions impact on local air quality. *Air Quality Atmosph Health.* 2013;6:295–305.
- [11] U.S. EPA, 2016. Available from: <https://www3.epa.gov/airquality/nitrogenoxides/health.html>.
- [12] Westerdahl D, Fruin S, Sax T, et al. Mobile platform measurements of ultrafine particles and associated pollutant concentrations on freeways and residential streets in Los Angeles. *Atmosph Environ.* 2005;39:3597–3610.
- [13] AirSensa, AirSensa. 2016. Available from: www.airsensa.org.
- [14] Smart Citizen, Smart Citizen Documentation. 2016. Available from: <http://docs.smartcitizen.me/>.
- [15] McConnell R, Islam T, Shankardass K, et al. Childhood incident asthma and traffic-related air pollution at home and school. *Environ Health Perspect.* 2010;118:1021–1026.
- [16] Vanos J. Childrens health and vulnerability in outdoor microclimates: a comprehensive review. *Environ Int.* 2015;76:1–15.
- [17] Pope RL. Spatiotemporal patterns, monitoring network design, and environmental justice of air pollution in the phoenix metropolitan region: a landscape approach; [PhD dissertation]. Arizona State University; 2014. Available from: http://search.proquest.com/openview/28bd668562758601e75f990f667e30a2/1?pq-origsite=gsc_holar&cbl=18750&diss=y.
- [18] Bales E, Nikzad N, Quick N, et al. Citsense: mobile air quality sensing for individuals and communities design and deployment of the citsense mobile air-quality system. Paper presented at: 2012 6th international conference on pervasive computing technologies for health-care (PervasiveHealth) and workshops, 2012; pp 155–158.
- [19] McKercher GR. Characteristics and applications of small, mobile air pollution monitors: a review. *Environ Pollut.* Forthcoming 2017. Available from: <http://www.science.direct.com/science/article/pii/S0269749116307321>
- [20] U.S. Census Bureau, 2015 Population Estimates. 2016. Available from: <http://factfinder.census.gov>.
- [21] Smart Citizen Kit – Field Evaluation. 2015. Available from: <http://www.aqmd.gov/docs/default-source/aq-spec/field-evaluations/smart-citizen-kit—field-evaluation.pdf?sfvrsn=2>.
- [22] e2v Technologies, MiCS-4514 Combined CO and NO2 Sensor Data Sheet. 2008. Available from: <http://files.manylabs.org/datasheets/MICS-4514.pdf>.
- [23] SGX Sensortech, Frequently asked questions for MiCS gas sensors. 2007. Available from: <https://www.cdiweb.com>.
- [24] Hasenfratz D, Saukh O, Sturzenegger S, et al. Participatory air pollution monitoring using smartphones. *Mobile Sens.* 2012:1–5.
- [25] Williams R. et al. Sensor evaluation report, 2014. Available from: <http://www.aqmd.gov/docs/default-source/aq-spec/resources-page/us-epa—sensor-evaluation-report.pdf?sfvrsn=0>
- [26] Weichenthal S, Kulka R, Dubeau A, et al. Traffic-related air pollution and acute changes in heart rate variability and respiratory function in urban cyclists. *Environmental Health Perspectives.* 2011;119:1373–1378.
- [27] Peters J, Van den Bossche J, Reggente M, et al. Cyclist exposure to UFP and BC on urban routes in Antwerp, Belgium. *Atmosph Env.* 2014;92:31–43.
- [28] Van den Bossche J, Peters J, Verwaeren J, et al. Mobile monitoring for mapping spatial variation in urban air quality: development and validation of a methodology based on an extensive dataset. *Atmosph Environ.* 2015;105:148–161.
- [29] Farrell W, Weichenthal S, Goldberg M, et al. Near roadway air pollution across a spatially extensive road and cycling network. *Environ Pollut.* 2016;212:498–507.
- [30] Vanos JK, Hebbert C, Cakmak S. Risk assessment for cardiovascular and respiratory mortality due to air pollution and synoptic meteorology in 10 Canadian cities. *Environ Pollut.* 2014;185:322–332.
- [31] Cao T, Thompson JE. Personal monitoring of ozone exposure: a fully portable device for under \$150 USD cost. *Sens Actuat B: Chem.* 2016;224:936–943.
- [32] Jiao W, Hagler GS, Williams RW, et al. Field assessment of the village green project: an autonomous community air quality monitoring system. *Environ Sci Technol.* 2015;49(10):6085–6092.
- [33] Devarakonda S, Sevusu P, Liu H, et al. Real-time air quality monitoring through mobile sensing in metropolitan areas. Paper presented at: Proceedings of the 2nd ACM SIGKDD international workshop on urban computing. 2013; p 15.
- [34] Bales E, Nikzad N, Ziftci C, et al. Personal pollution monitoring: mobile real-time air-quality in daily life Technical report, UCSD Computer Science Department; 2014. <http://cseweb.ucsd.edu/~earrowsm/TR.pdf>
- [35] Friedman MS, Powell KE, Hutwagner L, et al. Impact of changes in transportation and commuting behaviors during the 1996 Summer Olympic Games in Atlanta on air quality and childhood asthma. *Jama.* 2001;285:897–905.
- [36] Google Maps. 2016. Lubbock, TX. Map Underlay. Google Earth Maps, June 21, 2016.